Moroccan Journal of Chemistry
ISSN: 2351-812X
http://revues.imist.ma/?journal=morjchem&page=login
El-Bindary & al. / Mor. J. Chem. 8 N°4 (2020) 788-800

Box-Behnken design to enhance the corrosion resistance of high strength steel alloy in 3.5 wt.% NaCl solution

A. M. El-Shamy[(a)], M. A. El-Hadek[(b)], A. E. Nassef[(b,c)], R. A. El-Bindary[(b)]*

[(a)]Department of Physical Chemistry, Electrochemistry and Corrosion Lab, National Research Centre, El-Bohouth St. 33, Dokki, PO 12622, Giza, Egypt
[(b)]Department of Production and Mechanical Design Engineering, Faculty of Engineering, Port-Said University, Port-Said 42523, Egypt
[(c)]High Institute of Engineering and Technology, North Sinai, El-Arish, 45511, Egypt

** Corresponding author:*
ra.bindary@yahoo.com
Received 04 April 2020,
Revised 13 May 2020,
Accepted 05 Aug 2020

Abstract

Recently, the production of green corrosion inhibitors and green inhibition strategies is highly demanded in the field of science and technology due to the growing demand of green chemistry. Usage of plant extracts as metallic corrosion inhibitors has attracted considerable attention in the last few decades. Plant products are perfect green candidates for replacing traditional toxic corrosion inhibitors. Reduced environmental risk, lower cost, widespread availability and high corrosion inhibition efficiency make plant extracts ideal candidates for the substitution of costly and harmful traditional synthetic corrosion inhibitors. An aqueous extract of plant material Henna (Lawsonia Inermis) powder was used as a corrosion inhibitor to control the corrosion of high strength steel immersed in an aqueous solution containing 35000 ppm Cl^-, by electrochemical methods in the absence and presence of the inhibitor. Lawsone is the principal constituent of this plant extract. This has excellent efficiency in inhibition and displays excellent IE at neutral pH. Electro-chemical experiments such as potentiodynamic polarization and impedance were used to describe the mechanistic aspects of corrosion inhibitions. Box-Behnken method was used to investigate the effect of key parameters (i.e. concentration of inhibitors, temperature, and speed of rotation) on the efficiency of inhibition and corrosion rate of high strength steel alloy in 3.5 wt.% NaCl solutions. From electrochemical measurements and statistical analysis, it was found that the efficacy of inhibition improves with higher inhibitor concentration, low rotation speed and low temperature. The Lawsonia Inermis extracted demonstrated strong corrosion inhibition in saline media for high strength steel alloy and reached 81.68.

Keywords: *Lawsonia Inermis extract; Box-Behnken; High strength steel alloy; Electrochemical techniques*

1. Introduction

Corrosion is a natural and spontaneous process resulting in the conversion of pure metals and their alloys by chemical and/or electrochemical reactions with the surrounding environments into many stable forms such as sulfide, oxides, hydroxides etc. [1–3]. A very recent NACE 2016 report indicates that corrosion is causing a global economic loss of about 2.5 trillion US dollars, almost 3.4% of total GDP. However, the cost of corrosion can be decreased up to 15–35% (USD 375-875 billion) by applying current corrosion prevention technologies in a proper manner. Because of its connection with very high economic and safety losses, corrosion is a significant problem that must be tackled by scientists and engineers from around the world working in the field of corrosion and engineering [4–6]. Many methods of corrosion prevention have been developed, including the use of synthetic corrosion inhibitors due to their simplicity of synthesis and application and high efficacy at comparatively low concentration is one of the most popular and economical methods. Via their heteroatoms and π-electrons, these organic compounds adsorb metals and alloys over the surface and form protective surface barriers thereby shielding metals from corrosive degradation. Heteroatoms of organic inhibitors generally exist in polar useful groups such as –CN, $–NO_2$, $–NH_2$, –OH, $–OCH_3$, –COOH, $–COOC_2H_5$ etc., which act as centers of adsorption during the adsorption of these compounds on metal surfaces [7,8]. Such polar functional groups further improve the solubility of the compounds in the polar electrolytic media such as H_2O, HCl, H_2SO_4, HNO_3, H_3PO_4 etc. [9,10]. The use of traditional corrosion inhibitors in research, technology, and engineering is now limited due to the growing concept of green chemistry [11,12]. Green Chemistry is a branch of science and technology that utilizes a range of principles to mitigate the discharge of environmentally malignant materials into and design environmentally friendly chemicals [13,14]. Recently, the ecological awareness and stringent ecological regulations in all fields of science and technology have encouraged scientists and engineers working in the field of corrosion research to synthesize organic inhibitors by combining three or more reacting molecules in one stage with one phase multi-component reactions (MCRs) [15–17]. In addition, thorough consideration has also been given to the use of various plant extracts [18,19], chemical medicinal products (drugs) [20,21] and ionic liquids (designer chemicals) [22–24] for producing green corrosion inhibitors. Plants are characterized by their unique properties in transforming radiant energy (sunlight) into life which, through the photosynthesis process, provides organic compounds (carbohydrates). They are also a natural source of many raw materials in our everyday lives, such as fruit, fruits, plants, oils, resins and colorants. In such applications, plants are often characterized by their capacity during the photosynthesis cycle to continuously suck up "greenhouse" CO_2 emissions, highly toxic metals, and other contaminants, which is an important process from an environmental cleaning perspective. Revision of the literature indicates that few reviews for corrosion inhibition such as drugs have been published until today. Organic compounds and ionic liquids as inhibitors [25,26], inorganic corrosion inhibitors [27], food extracts as inhibitors [28], etc. The present research investigated the inhibition efficiency of an aqueous extract of plant material, Henna (Lawsonia Inermis) extract, in controlling the corrosion of high strength steel immersed in an aqueous solution containing 35000 ppm Cl^-, in the absence and presence of the inhibitor, using an electrochemical techniques for examining the effect of flow rate, inhibitor concentration and temperature on the inhibition efficiency. The optimum conditions among the variable parameters (i.e., concentration of inhibitor, rotation speed and temperature) which effect on the corrosion rates and inhibition efficiencies were tested by utilize of investigational arithmetical enterprise (Box-Behnken).

2. Materials and methods

2.1. Materials

Sodium chloride (NaCl, Merck, 96%), Lawsonia Inermis powder, absolute ethanol (C_2H_5OH, Merck, 99.9%), and acetone (C_3H_6O, Merck, 99.0%) were applied as customary. The high strength steel alloy substrate

with a quadrangular form with superficial proportions of 1x1 cm was laboring for the electrochemical assessments.

2.2. High Strength Steel Alloy

Inhibition possessions of Lawsonia Inermis extract **(**LI**)** were inspected on the high strength steel alloy electrode with a flag shape. High strength steel alloy electrode, which composed of 0.01% B, 0.03% C, 0.02% N, 0.01% Al, 0.17% Si, 0.01% P, 0.23% V, 1.50% Cr, 0.22% Mn, 0.01% Co, 3.20% Ni, 0.10% Cu, 0.60% Mo and the balance Fe, was used in this study. The equivalent carbon content of the steel alloy was calculated and found to be 0.781 [29]. The electrodes were graceful using SiC papers (several grades). The refined sample was wash away with bi-distilled water and formerly dried out. The destructive 3.5 wt.% NaCl solutions protected by LI at several concentrations were equipped by NaCl and bi-distilled water.

2.3. Preparation of Lawsonia Inermis Extract

Lawsonia Inermis extract (LI) was prepared previously [30] by dissolving 100 g/500 mL distilled water of Lawsonia Inermis powder in 1000 mL beaker, boiled for 30 min, then filtered and the filtrate is concentrated to 100 mL. The resulting clear solution was then used for preparing of the examination electrolytes in electrochemical studies. The major existing compound in aqueous extract of Lawsonia Inermis is 2-Hydroxy-1,4-napthoquinone [31]. The electrodes were graceful using SiC papers (several grades). The refined sample was wash away with bi-distilled water and formerly dried out. The destructive 3.5 wt.% NaCl solutions protected by LI at several concentrations were equipped by NaCl and bi-distilled water.

2.4. Electrochemical Measurements

The electrochemical investigations were applied by means of conservative three electrodes in a tube-shaped Pyrex glass cell. The high-resistance steel electrodes with an exposed area of 1 cm^2 were used as working electrodes. The platinum electrode and Ag/AgCl were independently used as an auxiliary and as the reference electrode. The electrochemical measurements were used meticulously by Volta-Master 4 programming on the Volta-Lab PGZ402 potentiostat. Before performing the electrochemical investigations, the high-resistance steel electrodes were immersed in a 3.5 wt.% NaCl solution without and with different inhibitor loads for 30 min to create a steady state open circuit (E_{ocp}) potential. The potentiodynamic polarization curves were obtained by scanning the potential in the forward direction from –1.0 V to –0.2 V vs. Ag/AgCl at a scan rate of 0.001 V/s. In addition, the (EIS) experiments were conducted at open circuit potential with an amplitude of 10 mV using AC signal between the maximum frequency limit of 100 kHz and lowest frequency limit of 0.03 Hz. Simulation ZSimpWin 3.60, equivalent circuit software, evaluated the impedance data and fitted it with [32–36].

2.5. Statistical Analysis

For studying the corrosion rate and inhibition efficiency of high strength steel alloy using of LI as inhibitor, Box–Behnken experimental design [37,38] for the variables (concentration of inhibitor, rotation speed and temperature) is shown in Table 1. The response variables were developed by design of the rejoinder superficial outlines and the greatest analytical replicas. The Box–Behnken enterprise can acceptable the subsequent prototypical formula [39]:

$$E(y) = \beta_0 \sum_{i=1}^{3} \beta_i X_i + \sum_{i=1}^{3} \sum_{j=1}^{3} \beta_{ij} X_i X_j \qquad (1)$$

where y is the rejoinder adjustable estimation, X_i's are the autonomous parameters (inhibitor load, rotation speed and temperature) that are recognized for each experimental run, and β_0, β_i, and β_{ij} are the worsening limits. Software bundle, Design-Expert 6.1, Stat–Ease, Inc., Minneapolis, USA, was castoff for deterioration examination of investigational statistics and to design rejoinder superficial. The statistical parameters were subjected to approximate the variance analysis (ANOVA). The amount of appropriate the investigational consequences to the polynomial prototypical calculation was articulated to determinate the coefficient, R^2.

Table 1. Corrosion rate and inhibition efficiency of high strength steel alloy in 3.5 wt.% NaCl**.**

Run Number	Conc. of Inhibitor (%)	Rotation Speed (rpm)	Temp. (°C)	Thrust Pressure (Pa)	Time (s)	CR, (mL/Y)	I. E., (%)
1	5	150	50	101325	1200	9.21	42.07
2	10	150	50	101325	1200	6.6	58.49
3	5	250	50	101325	1200	11.6	29.69
4	10	250	50	101325	1200	7.8	56.42
5	5	200	25	101325	1200	8.4	49.09
6	10	200	25	101325	1200	4.5	72.73
7	5	200	75	101325	1200	12.4	24.84
8	10	200	75	101325	1200	10.86	34.18
9	7.5	150	25	101325	1200	4.24	73.33
10	7.5	250	25	101325	1200	6.23	65.20
11	7.5	150	75	101325	1200	10.2	35.03
12	7.5	250	75	101325	1200	12.79	28.54
13	7.5	200	50	101325	1200	9.47	42.60
14	7.5	200	50	101325	1200	9.47	42.60
15	7.5	200	50	101325	1200	9.47	42.60
16	7.5	200	50	101325	1200	9.47	42.60
17	7.5	200	50	101325	1200	9.47	42.60

Blank corrosion rate (150 rpm = 53.9 mpy), (200 rpm = 55.2 mpy) and (250 rpm = 57.9 mpy).

3. Results and Discussion

3.1. Electrochemical Measurements

3.1.1. Open Circuit Potential

The action of corrosion from high strength steel and the penetrability of the surface layer can be obtained by the measurements of open circuit potential (OCP). The time-dependent variation of high strength steel OCP submerged in 3.5 wt.% NaCl solution, without and with LI inhibitor concentrations, is shown in Fig. 1. The OCP values were observed to change in a positive direction. This suggests that in the presence of the LI inhibitor, the kinetics of the anodic reaction of high strength steel in solution 3.5 wt.% NaCl is more strongly affected. This behavior suggests the formation of a protective layer due to the adsorption on the metal surface of the inhibitor molecules which decreases the active sites of the high strength steel surface. Nevertheless, the change in OCP curves between the inhibitor's absence and presence is less than 85 mV which suggests that the inhibitor being investigated is a mixed-type inhibitor.

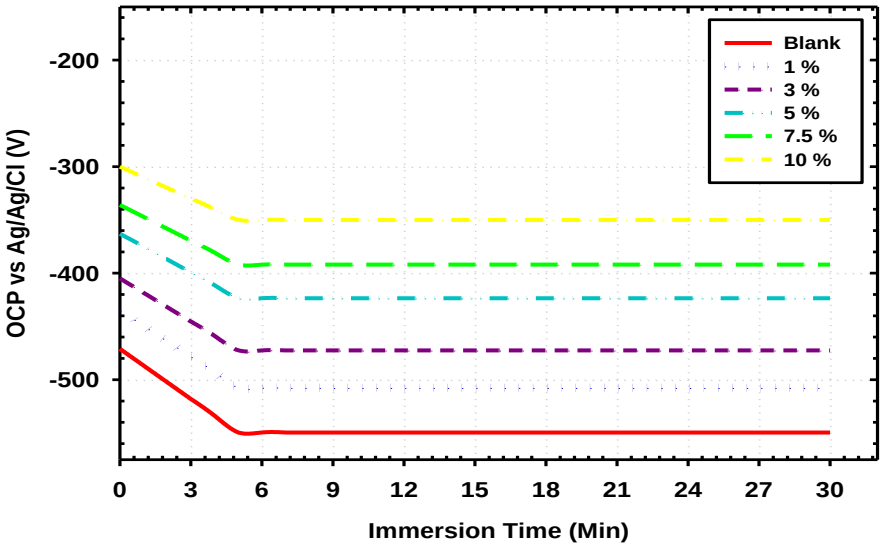

Figure 1. Open circuit potential versus time of high strength steel alloy sample engrossed in 3.5 wt. % NaCl media and various loads of LI.

3.1.2. Potentiodynamic Polarization Measurements

Potentiodynamic polarization analysis was performed to correspondingly discern the effect of the inhibitor on the anodic dissolution of high strength steel and the reduction of cathodic oxygen. Table 2 shows the polarization parameters of steel electrode when Lawsonia Inermis is present and absent. Due to its notable changes in the anodic Tafel branch, b_a value, Lawsonia Inermis has been believed to function as an anodic inhibitor. The adsorption of Lawsonia Inermis on the surface of steel alloy limited the corrosion cycle by blocking the reaction site of the metal surface and thus reducing the b_a value. A graphical data as shown in Fig. 2 shows a marked change in the cathodic Tafel branch, b_c, to lower corrosion current density values. The oxygen reduction mechanism occurs at the cathodic region which subsequently induces the b_c shift. The modifications in b_c are well known to explain the alteration of the cathodic reaction mechanism. The second supposition was therefore made that Lawsonia Inermis functions as a cathodic inhibitor.

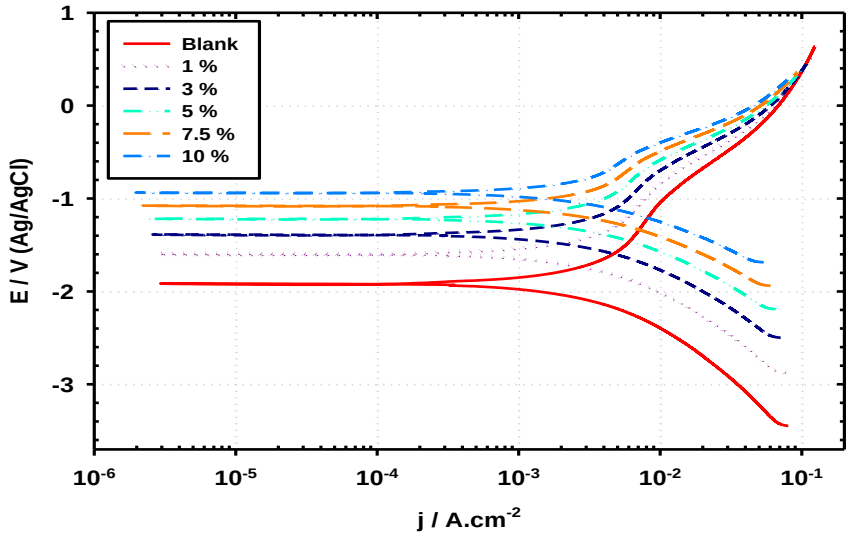

Figure 2. Potentiodynamic polarization strategies of high strength steel alloy sample enthralled in 3.5 wt. % NaCl medium and assorted loads of LI.

Table 2. Corrosion parameters obtained from the PD measurements for high strength low alloy which immersed in absence and in the presence of different concentration of LI.

Medium	Parameters						
	B_c mV dec^{-1}	E_{corr} mV	j_{corr} μAcm^{-2}	B_a mV dec^{-1}	R_p Ωcm^2	R_{corr} mmy^{-1}	IE %
Blank	-91.32	-550.62	2821	71.5	3.91	29.14	–
1 %	-86.51	-509.2	2553	75.1	4.7	22.4	23.02
3 %	-83.88	-473.8	2476	79.6	5.8	15.1	48.42
5 %	-81.20	-423.2	2401	81.2	7.7	12.1	58.75
7.5 %	-79.32	-392.9	2281	86.1	9.6	9.1	69.90
10 %	-74.84	-349.8	2064	94.2	12.9	6.3	78.34

3.1.3. Electrochemical Impedance Spectroscopy (EIS) Measurements

EIS was used to test the signature impedance as well as the capacitance activity in the presence and absence of LI. The calculation of the EIS was carried out using alternating current (AC) impedance calculation signals with respect to the open circuit potential (OCP). All the referred potential was connected to the reference electrode (Ag/AgCl). The impedance measurements used a frequency range of 1 kHz down to 10mHz. The findings were evaluated using fit program. Table 3 displays the resistance values to charge transfer and double layer capacitance. The data shows that coated samples integrated with henna provided higher resistance to transfer charges (R_{ct}) compared to bare metal. The highest resistance obtained in this research is the coated sample with 10 percent coating of the henna extract. Fig. 3 depicts the Nyquist plot with and without the coating. It can be shown that the coated coupon with 0 percent henna extract shows the smallest half-circle, followed by a coated coupon integrated with 5 percent henna extract. 10 percent henna extract represents the largest semicircle. The demi-circle size contributes to the degree of resistance to corrosion. The greater half-circle shows a greater degree of resistance. Rising R_{ct} value with the addition of henna extract percentage gave better performance in retarding corrosion due to oxide layer formation [40]. A high antioxidant activity of henna has led to increased electrical resistance on the surface of aluminum [41]. This shows that the corrosion resistance often improves as a proportion of henna extracts improves, and the corrosion rate decreases. In addition, the high impedance value of the coating is related to the formation of the deposited layer and consequently slows the rate of penetration of electrolytes into the coating [42].

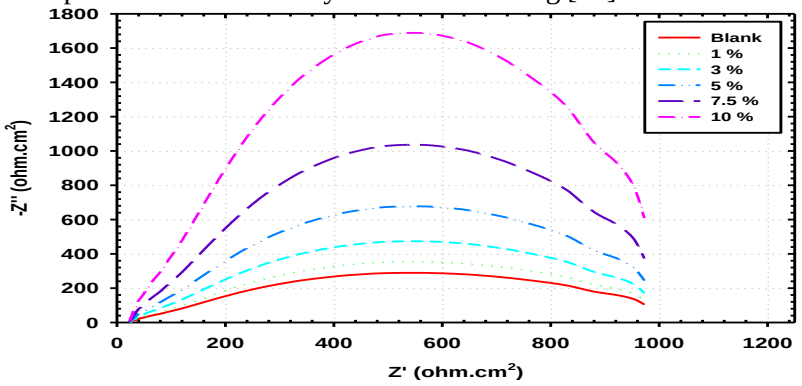

Figure 3. Nyquist plots for high strength steel alloy sample engrossed in 3.5 wt. % NaCl electrolyte and various loads of LI.

Table 3. Parameters obtained by fitting the EIS data with the equivalent circuit for high strength low alloy which immersed in absence and in the presence of different concentration of LI.

Medium	Parameters						
	$R_s/\Omega\ cm^2$	Yo/F cm^2	n	$R_{p1}/\ \Omega\ cm^2$	$R_{p2}/\Omega\ cm^2$	L/H	I.E., %
Blank	1.45	0.0013	74.65	345	2.98	17.534	–
1 %	1.52	0.0012	0.90	390	4.30	18.116	13.1
3 %	1.92	0.0011	0.92	485	5.78	19.929	40.5
5 %	2.38	0.0011	0.95	680	7.72	21.324	67.1
7.5 %	3.16	0.0010	0.95	1020	9.6	23.679	86.4
10 %	3.54	0.0008	0.98	1700	11.5	25.721	91.7

3.2. Statistical Analysis

3.2.1. Optimization of the experimental conditions

To optimize the three individual factors (inhibitor concentration, rotation speed and temperature), there were a total of 17 experimental runs in the Box-Behnken design Table 1.

3.2.2. Corrosion rate

Fig. 4 shows the contour plot of the consequence of inhibitor concentration and rotation speed on the corrosion rate of high strength steel alloy at different temperatures 25, 50 and 75 °C. It is clear that, at 25 °C the corrosion rate was decreased from 8.26 to 3.35 % with increasing inhibitor concentration from 5 to 10 %. Also, the effect of increasing rotation speed from 150 to 250 rpm, indicating a little effect. By increasing temperature to 50 and/or 75 °C, the corrosion rate increases with increasing inhibitor concentration and insignificant effect with rotation speed. The contour plot of the consequence of inhibitor concentration and temperature on the corrosion rate of high strength steel alloy at different rotation speed 150, 200 and 250 rpm showed that, at 150 rpm the corrosion rate has a little effect with increasing inhibitor concentration from 5 to 10 %. Also, increasing temperature from 25 to 75 °C increases the corrosion rate from 4.05 to 10.42 %. By increasing rotation speed to 200 and/or 250 rpm, the corrosion rate increases with increasing temperature and insignificant effect with inhibitor concentration. The contour plot of the consequence of rotation speed and temperature on the corrosion rate of high strength steel alloy at different concentration of inhibitor 5, 7.5 and 10 % showed that, at 5 % the corrosion rate was increased from 7.03 to 13.25 % with increasing temperature from 25 to 75 °C. Also, by increasing inhibitor concentration from 5 to 10 %, indicating a little effect. By increasing inhibitor concentration to 7.5 and/or 10%, the corrosion rate decreases with increasing temperature and insignificant effect with inhibitor concentration.

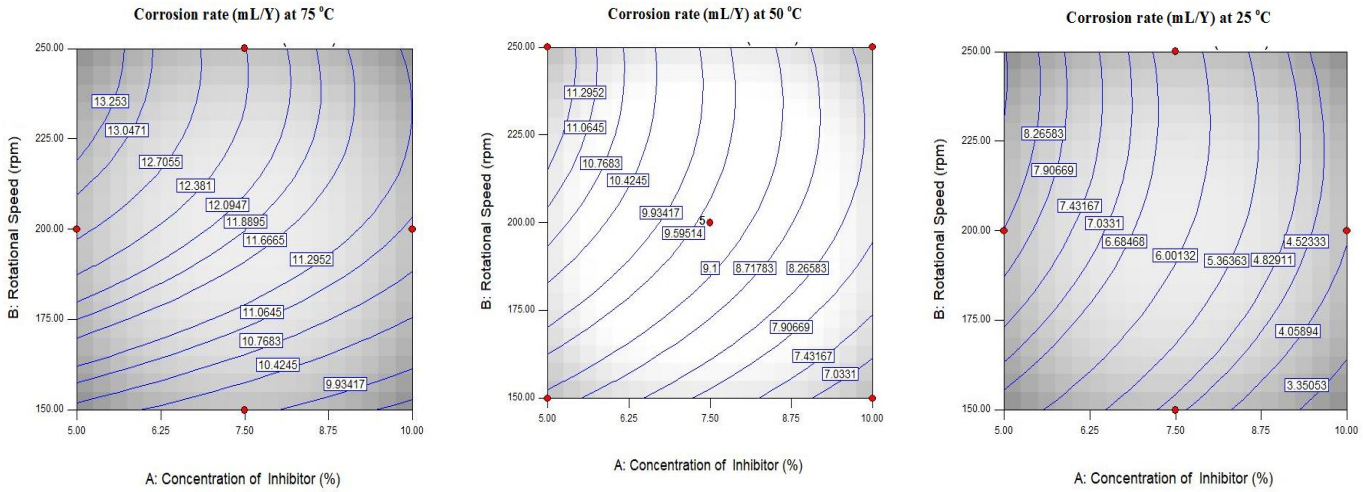

Figure 4. Contour plot of corrosion rate as a purpose of inhibitor load and rotational speed at the temperatures 25, 50 and 75 ºC.

Fig. 5 shows the 3D plot of corrosion rate of high strength steel alloy as a function of inhibitor concentration and rotation speed at different temperatures 25, 50 and 75 ºC. It shows that, at 25 ºC the maximum corrosion rate was 8.75 mL/Y. Also, increasing the temperature from 50 to 75 ºC increases the maximum corrosion rate to 11.60 and 13.58 mL/Y, respectively. The 3D plot of the consequence of temperature and inhibitor load on the deterioration rate of high strength steel alloy at different rotation speed 150, 200 and 250 rpm showed that, at 150 rpm the maximum corrosion rate was 10.65 mL/Y. Also, increasing the rotation speed from 200 to 250 shows insignificant increases the maximum corrosion rate to 12.79 and 13.58 mL/Y, respectively [43]. The 3D plot of corrosion rate of high strength steel alloy as a function of rotation speed and temperature at different inhibitor concentration 5, 7.5 and 10 % showed that, at 5 % the maximum corrosion rate was 10.30 mL/Y. Also, increasing the inhibitor concentration from 7.5 to 10 % decreases the maximum corrosion rate to 10.00 and 9.18 mL/Y, respectively.

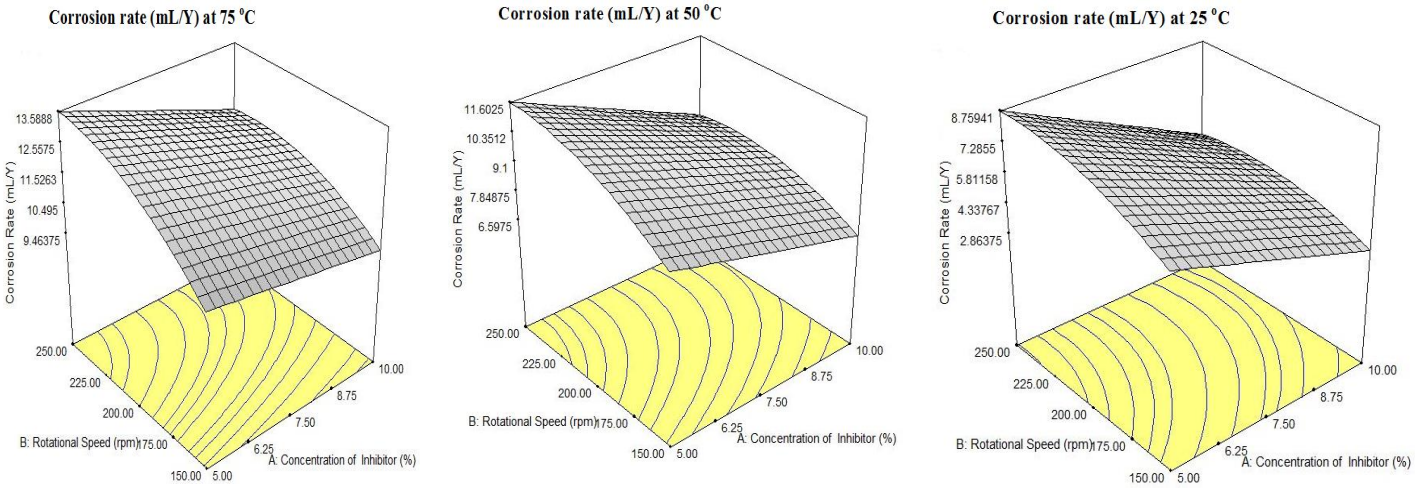

Figure 5. 3D plot of corrosion rate as a function of inhibitor concentration and rotation speed at temperature 25, 50 and 75 ºC.

All the investigational data, composed at the 3D cubic as publicized in Fig. 6, exposed that the corrosion rate which fluctuated from 2.86 to 13.59 mL/Y can be produced. The lowest corrosion rate, 2.86 mL/Y, can be obtained at high concentration of inhibitor and small stages of temperature and rotation speed. On the other hand, the highest corrosion

rate can be achieved at low concentration of inhibitor and high levels of temperature and rotation speed. However, increasing the concentration of inhibitor leads to decrease the corrosion rate which is desirable. This is attributed to the LI inhibitor, which is well known as inhibiting agent, since it stable at < 50 °C and 150 rpm. Fig. 7 displays the normal plot of residuals in which almost all the residuals fall on a straight line, reflecting that errors were expected to distribute normally. Namely, the model exhibits a good stability to predict the response.

Final equation in terms of actual factors indicated as follows:

Corrosion Rate (mL/Y) = -7.16250

*Concentration of Inhibitor (%) = - 0.59750

*Rotational Speed (rpm) = + 0.13967

*Temperature (°C) = + 0.089000

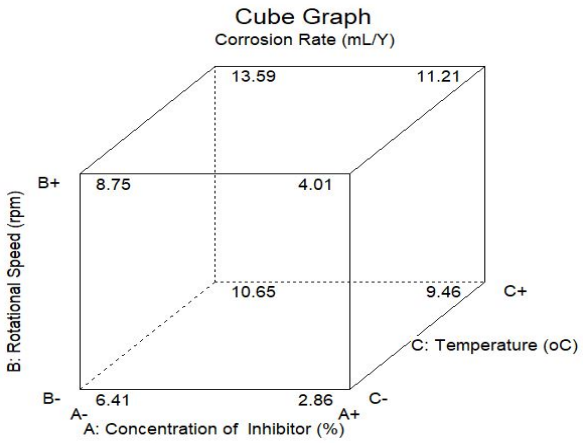

Figure 6. 3D plot of corrosion rate as a purpose of inhibitor load, rotation speed, and temperature variables.

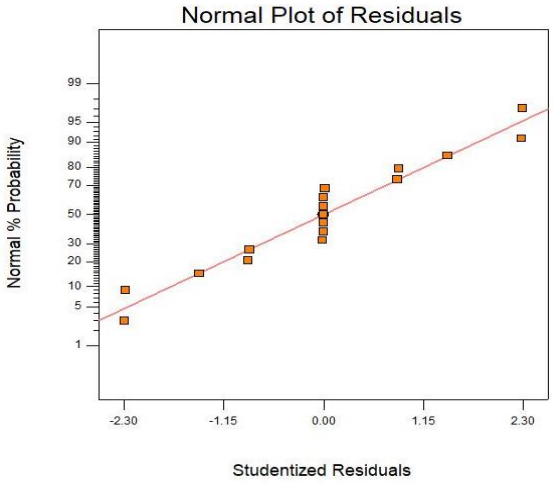

Figure 7. Normal plot of error distribution for corrosion rate.

3.2.3. Inhibition efficiency

Fig. 8 shows the contour plot of the effect of inhibitor concentration and rotation speed on the inhibition efficiency of high strength steel alloy at different temperatures 25, 50 and 75 °C. At 25 °C the inhibition efficiency was increased from 52.76 to 79.35 % with increasing inhibitor concentration from 5 to 10 %. Also, increasing rotation speed from 150 to 250 rpm, decreases the inhibition efficiency a little. By increasing temperature to 50 and/or 75 °C, the inhibition efficiency decreases with increasing inhibitor concentration and rotation speed. The contour plot of the consequence of

inhibitor concentration and temperature on the inhibition efficiency of high strength steel alloy at different rotation speed 150, 200 and 250 rpm showed that, at 150 rpm the inhibition efficiency was increased a little with increasing inhibitor concentration from 5 to 10 %. Also, increasing temperature from 25 to 75 ^{o}C increases the inhibition efficiency from 73.60 to 34.88 %, indicating no effect. By increasing rotation speed to 200 and/or 250 rpm, the inhibition efficiency decreases with increasing inhibitor concentration and temperature. The contour plot of the consequence of rotation speed and temperature on the inhibition efficiency of high strength steel alloy at different concentration of inhibitor 5, 7.5 and 10% showed that, at 5% the inhibition efficiency was decreased from 52.76 to 21.73 % with increasing temperature from 25 to 75 ^{o}C. Also, increasing rotation speed from 150 to 250 rpm, decreases the inhibition efficiency a little. By increasing inhibitor concentration to 7.5 and/or 10%, the inhibition efficiency increases with increasing rotation speed and temperature.

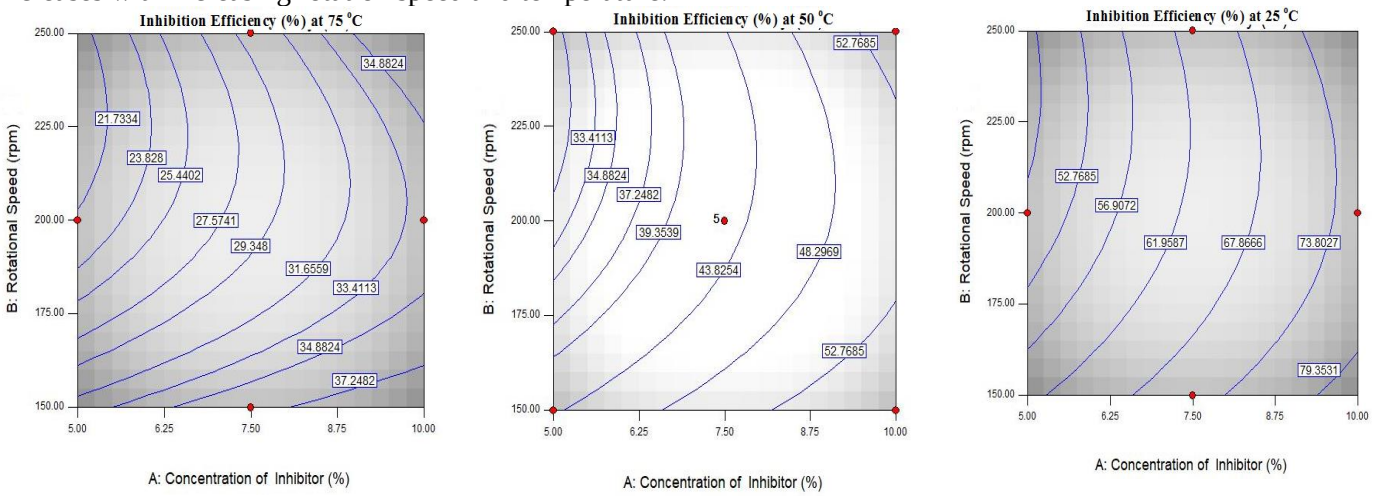

Figure 8. Contour plot of inhibition efficiency as a purpose of inhibitor load and rotational speed at the temperatures 25, 50 and 75 ^{o}C.

Fig. 9 shows the 3D plot of the inhibition efficiency of high strength steel alloy as a purpose of inhibitor load and rotation speed at diverse temperatures 25, 50 and 75 ^{o}C. It shows that, at 25 ^{o}C the maximum inhibition efficiency was 47.00 %. Also, increasing the temperature from 50 to 75 ^{o}C decreases the inhibition efficiency to 30.41 and 20.25 %, correspondingly. The 3D plot of the inhibition efficiency of high strength steel alloy as a purpose of inhibitor load and temperature at diverse rotation speed 150, 200 and 250 rpm showed that, at 150 rpm the maximum inhibition efficiency was 32.54 %. Also, increasing the rotation speed from 200 to 250 rpm shows insignificant increases the inhibition efficiency to 22.04 and 20.93 %, respectively. The 3D plot of the inhibition efficiency of high strength steel alloy as a purpose of rotation speed and temperature at diverse inhibitor concentration 5, 7.5 and 10 % showed that, at 5 % the inhibition efficiency was 32.50 %. Also, increasing the temperature from 7.5 and 10 % increases the maximum inhibition efficiency to 36.00 and 39.00 %, correspondingly. All the investigational data, composed at the 3D cubic as given away in Fig. 10, exposed that the inhibition efficiency which fluctuated from 20.94 to 81.68 (%) can be produced. The lowest inhibition efficiency, 20.94 %, can be obtained at low concentration of inhibitor and high levels of temperature and rotation speed. On the other hand, the highest inhibition efficiency can be realized at great concentration of inhibitor and small stages of temperature and rotation speed [44-46]. However, growing the load of inhibitor leads to increase the inhibition efficacy which is desirable. This is attributed to the LI inhibitor, which is well known as inhibiting agent, since it stable at < 50 ^{o}C and 150 rpm. Fig. 11 displays the normal plot of residuals in which almost all the residuals fall on a straight line, reflecting that errors were expected to distribute normally. Namely, the model exhibits a good stability to predict the response.

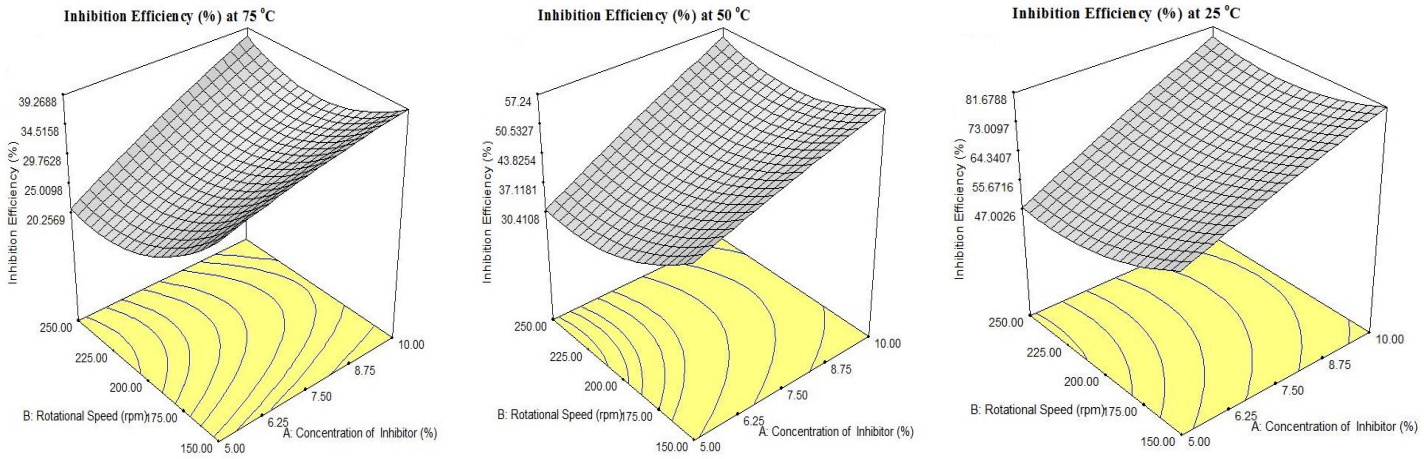

Figure 9. 3D plot of inhibition efficiency as a function of inhibitor concentration and rotation speed at temperature 25, 50 and 75 ºC.

Final equation in terms of actual factors: Inhibition Efficiency (%) = + 158.16750

* Concentration of Inhibitor (%) = + 4.03950

* Rotational Speed (rpm) = - 0.99432

* Temperature (ºC) = - 0.84280

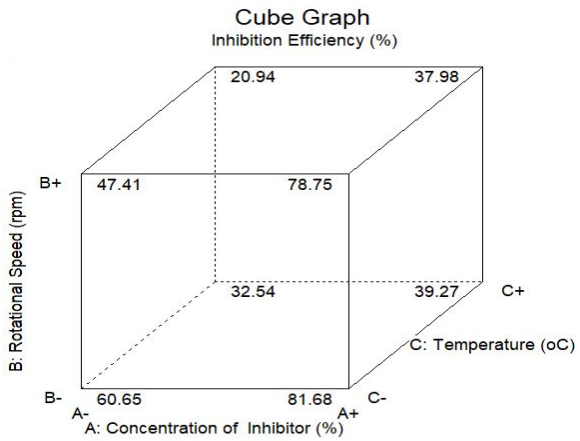

Figure 10. 3D plot of inhibition efficiency as a function of inhibitor concentration, rotation speed, and temperature variables.

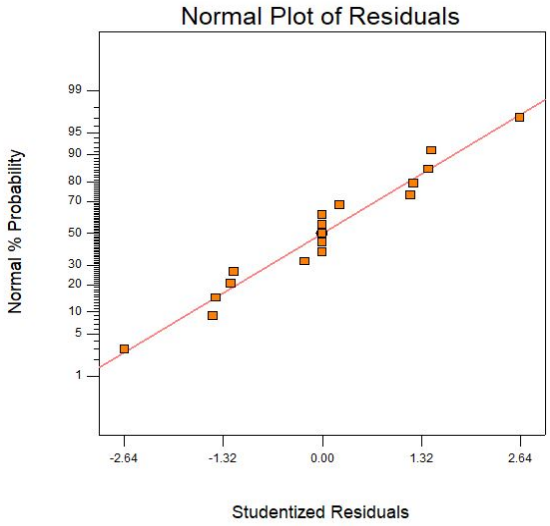

Figure 11. Normal plot of error distribution for inhibition efficiency.

4. Conclusion

The LI extract functions in the way of defensive coating process as an excellent inhibitor. The highest amount of LI extract produces the most resistant layer and does less corroding to the coupon. It is found that, 10 % LI extract provides the lowest corrosion rate compared to unprotected steel surface. The electrochemical techniques curves show a high efficiency in all trials depending on the LI concentration, since the inhibition efficiency increases with increase of inhibitor loads. Lawsone is constitutes the major constituents of LI inhibitor, it was found to be an efficient corrosion inhibitor of high strength steel in 3.5 wt.% NaCl solutions. The results were also show that, with decreasing temperature and flow rate, the inhibition efficiency increased. These data were also proved by EIS results, since the inhibitor was found to enhance the resistance of charge transfer, R_{ct}, as the concentration increases. Finally, LI is a potential green material to be produced in marine environment as a corrosion inhibitor to high strength steel alloy. It is due to heteroatoms such as oxygen and hydrogen that are active centers for the process of adsorption process on the steel surface. The inhibitor inhibits the corrosion cycle excellent and at this concentration the maximum inhibition efficiency is achieved. Lawsonia Inermis 10% is also the highest concentration to be used as a corrosion agent for high strength steel alloy in seawater. The statistical analysis planned trials produced on the Box–Behnken method were castoff to evaluate the percentage of effectiveness deterioration in the presence of LI as inhibitor.

References

[1] W. Mai, S. Soghrati, R. G. Buchheit, *Corr. Sci*., 110 (2016) 157-166.

[2] N. Kıcır, G. Tansuğ, M. Erbil, T. Tüken, *Corr. Sci*., 05 (2016) 88-99.

[3] P. Singh, V. Srivastava, M. Quraishi, *J. Mol. Liq*., 216 (2016) 164-173.

[4] Z. Hu, Y. Meng, X. Ma, H. Zhu, J. Li, C. Li, D. Cao, (2016). Experimental and theoretical studies of benzothiazole derivatives as corrosion inhibitors for carbon steel in 1 M HCl, Corr. Sci., 112: 563-575.

[5] J. Haque, V. Srivastava, C. Verma, M. Quraishi, *J. Mol. Liq*., 225 (2017) 848-855.

[6] S. R. Kumar, I. Danaee, M. RashvandAvei, M. Vijayan, *J. Mol. Liq*., 212 (2015) 168-186.

[7] X. Li, X. Xie, S. Deng, G. Du, *Corr. Sci*., 87 (2014) 27-39.

[8] C. Verma, L. Olasunkanmi, E.E. Ebenso, M. Quraishi, *J. Mol. Liq*., 251 (2017) 100-118.

[9] C. Verma, E.E. Ebenso, M. Quraishi, *J. Mol. Liq*., 248 (2017) 927-942.

[10] E. M. Sherif, A. T. Abbas, H. Halfa, A. M. El-Shamy, *Int. J. Electrochem. Sci*., 10 (2015) 1777-1791.

[11] S. A. Umoren, U. M. Eduok, *Carbohyd. Poly*., 140 (2016) 314-341.

[12] K. Hu, J. Zhuang, C. Zheng, Z. Ma, L. Yan, H. Gu, X. Zeng, J. Ding, *J. Mol. Liq*., 222 (2016) 109-117.

[13] R. Mohammadinejad, S. Karimi, S. Iravani, R.S. Varma, *Green Chem*., 18 (2016) 20-52.

[14] R. S. Varma, *Green Chem*., 16 (2014) 2027-2041.

[15] R. C. Cioc, E. Ruijter, R.V. Orru, *Green Chem*., 16 (2014) 2958-2975.

[16] A. Aljuhani, W.S. El-Sayed, P.K. Sahu, N. Rezki, M.R. Aouad, R. Salghi, M. Messali, *J. Mol. Liq*., 249 (2018) 747-753.

[17] G. Ameta, A.K. Pathak, C. Ameta, R. Ameta, P.B. Punjabi, *J. Mol. Liq*., 211 (2015) 934-937.

[18] E. Alibakhshi, M. Ramezanzadeh, G. Bahlakeh, B. Ramezanzadeh, M. Mahdavian, M. Motamedi, *J. Mol. Liq*., 255 (2018) 185-198.

[19] P. Parthipan, J. Narenkumar, P. Elumalai, P.S. Preethi, A.U.R. Nanthini, A. Agrawal, A. Rajasekar, *J. Mol. Liq*., 240 (2017) 121-127.

[20] I. B. Obot, E. E. Ebenso, M. M. Kabanda, *J. Environ. Chem. Eng*., 1 (2013) 431-439.

[21] S. Mo, L. J. Li, H. Q. Luo, N. B. Li, *J. Mol. Liq*., 242 (2017) 822- 830.

[22] S. Yesudass, L.O. Olasunkanmi, I. Bahadur, M.M. Kabanda, I. Obot, E.E. Ebenso, *J. Taiwan Inst. Chem. Eng*., 64 (2016) 252-268.
[23] F. El-Hajjaji, M. Messali, A. Aljuhani, M. Aouad, B. Hammouti, M. Belghiti, D. Chauhan, M. Quraishi, *J. Mol. Liq*., 249 (2018) 997-1008.
[24] S. K. Shetty, A. N. Shetty, *J. Mol. Liq*., 225 (2017) 426-438.
[25] M. Goyal, S. Kumar, I. Bahadur, C. Verma, E. E. Ebenso, *J. Mol. Liq*., 256 (2018) 565-573.
[26] S. A. Umoren, M. M. Solomon, *J. Environ. Chem. Eng*., 5 (2017) 246-273.
[27] M. Antonijevic, M. Petrovic, *Int. J. Electrochem. Sci*., 3 (2008) 1-28.
[28] M. Chaussemier, E. Pourmohtasham, D. Gelus, N. Pécoul, H. Perrot, J. Lédion, H. Cheap-Charpentier, O. Horner, *Desalin*., 356 (2015) 47-55.
[29] M. Bruneau, C.M. Uang, A. Whittaker, Ductile Design of Steel Structures, McGraw Hill, New York, 1997.
[30] A. M. El-Shamy, M. A. El-Hadek, A. E. Nassef, R. A. El-Bindary, *J. Chem*., (2020) Article ID 9212491.
[31] D. B. Tripathy, M. Murmu, P. Banerjee, and M. A. Quraishi, *Desalin*., 472 (2019) 114-128.
[32] M. F. Shehata, A. M. El-Shamy, K. M. Zohdy, E. S. M. Sherif, and S. Zein El Abedin, *Appl. Sci*., 10 (2020) 1444-1453.
[33] K. M. Zohdy, A. M. El-Shamy, A. Kalmouch, and E. A. M. Gad, *Egypt. J. Petroleum*, 28 (2019) 355-359.
[34] Y. Reda, A. M. El-Shamy, A. K. Eessaa, *Ain Shams Eng. J*., 9 (2018) 2973-2982.
[35] Y. Reda, K. M. Zohdy, A. K. Eessaa, A. M. El-Shamy, *Egypt. J. Chem*., 63 (2020) 579-597.
[36] Y. Reda, A. M. El-Shamy, K. M. Zohdy, A. K. Eessaa, *Ain Shams Eng. J*., 11 (2020) 191–199.
[37] S. Elavarasan, M. Gopalakrishnan, *Spectrochim. Acta A*, 133 (2014) 1-6.
[38] J. A. Cornell, D. C. Montgomery, *J. Qual. Technol*. 28 (1996) 163-176.
[39] M. Wang, Z. Zhou, Q. Wang, Y. Liu, Z. Wang, X. Zhang, *Res. Phys*., 15 (2019) 102708.
[40] F. Gapsari, R. Soenoko, A. Suprapto, and W. Suprapto, *Int. J. Corr*., (2015) Article ID 567202.
[41] E. Akbarinezhad, F. Rezaei, and J. Neshati, *Prog. Org. Coat*., 61 (2008) 45-52.
[42] A. Al-Borno, X. Chen, and S. K. Dhoke, *Int. J. Corr*., (2015) Article ID 903478.
[43] S. D. Accelrys, Software Inc., (2009).
[44] Z. Salarvand, M. Amirnasr, M. Talebian, K. Raeissi, S. Meghdadi, *Corr. Sci*., 114 (2017) 133-145.
[45] A. Mansri, B. Bouras, Mor. J. Chem. 2 N°4 (2014) 252-271
[46] R. Tolulope Loto, C. Akintoye Loto, A. Lukman Olaitan, P. Babalola, Mor. J. Chem. 5 N°1 (2017) 81-95